Journal of Orthopaedic Translation (2018) 12, 55—65

Available online at www.sciencedirect.com

ScienceDirect

journal homepage: http://ees.elsevier.com/jot

ORIGINAL ARTICLE

Finite element analysis of biomechanical effects of total ankle arthroplasty on the foot

Yan Wang [a,b], Zengyong Li [c], Duo Wai-Chi Wong [a,b], Cheng-Kung Cheng [d], Ming Zhang [a,b,*]

[a] *Department of Biomedical Engineering, Faculty of Engineering, The Hong Kong Polytechnic University, Hong Kong, China*
[b] *The Hong Kong Polytechnic University Shenzhen Research Institute, Shenzhen, China*
[c] *The National Research Center for Rehabilitation Technical Aids, Beijing, China*
[d] *Key Laboratory for Biomechanics and Mechanobiology of Ministry of Education, Beihang University, Beijing, China*

Received 25 August 2017; received in revised form 8 December 2017; accepted 11 December 2017
Available online 30 December 2017

KEYWORDS
Ankle prosthesis;
Bone stress;
Finite element analysis;
Joint contact pressure;
Plantar pressure;
Total ankle arthroplasty

Abstract *Background:* Total ankle arthroplasty is gaining popularity as an alternation to ankle arthrodesis for end-stage ankle arthritis. Owing to the complex anatomical characteristics of the ankle joint, total ankle arthroplasty has higher failure rates. Biomechanical exploration of the effects of total ankle arthroplasty on the foot and ankle is imperative for the precaution of postoperative complications. The objectives of this study are (1) to investigate the biomechanical differences of the foot and ankle between the foot with total ankle arthroplasty and the intact foot and (2) to investigate the performance of the three-component ankle prosthesis.
Methods: To understand the loading environment of the inner foot, comprehensive finite element models of an intact foot and a foot with total ankle arthroplasty were developed to simulate the stance phase of gait. Motion analysis on the model subject was conducted to obtain the boundary and loading conditions. The model was validated through comparison of plantar pressure and joint contact pressure between computational prediction and experimental measurement. A pressure mapping system was used to measure the plantar pressure during balanced standing and walking in the motion analysis experiment, and joint contact pressure at the talonavicular joint was measured in a cadaver foot.
Results: Plantar pressure, stress distribution in bones and implants and joint contact loading in the two models were compared, and motion of the prosthesis was analysed. Compared with the intact foot model, averaged contact pressure at the medial cuneonavicular joint increased

* Corresponding author. Department of Biomedical Engineering, Faculty of Engineering, The Hong Kong Polytechnic University, Hong Kong, China.
E-mail addresses: annie.wang@connect.polyu.hk (Y. Wang), zyongli@sdu.edu.cn (Z. Li), duo.wong@polyu.edu.hk (D.W.-C. Wong), zhengchenggong@buaa.edu.cn (C.-K. Cheng), ming.zhang@polyu.edu.hk (M. Zhang).

https://doi.org/10.1016/j.jot.2017.12.003
2214-031X/© 2017 The Authors. Published by Elsevier (Singapore) Pte Ltd on behalf of Chinese Speaking Orthopaedic Society. This is an open access article under the CC BY-NC-ND license (http://creativecommons.org/licenses/by-nc-nd/4.0/).

by 67.4% at the second-peak instant. The maximum stress in the metatarsal bones increased by 19.8% and 31.3% at the mid-stance and second-peak instants, respectively. Force that was transmitted in three medial columns was 0.33, 0.53 and 1.15 times of body weight, respectively, at the first-peak, mid-stance and second-peak instants. The range of motion of the prosthetic ankle was constrained in the frontal plane. The lateral side of the prosthesis sustained higher loading than the medial side.

Conclusion: Total ankle arthroplasty resulted in great increase of contact pressure at the medial cuneonavicular joint, making it sustain the highest contact pressure among all joints in the foot. The motion of the prosthesis was constrained in the frontal plane, and asymmetric loading was distributed in the bearing component of the ankle prosthesis in the mediolateral direction.

The translational potential of this article: Biomechanical variations resulted from total ankle arthroplasty may contribute to negative postoperative outcomes. The exploration of the biomechanical performance in this study might benefit the surgeons in the determination of surgical protocols to avoid complications. The analysis of the performance of the ankle prosthesis could enhance the knowledge of prosthetic design.

© 2017 The Authors. Published by Elsevier (Singapore) Pte Ltd on behalf of Chinese Speaking Orthopaedic Society. This is an open access article under the CC BY-NC-ND license (http://creativecommons.org/licenses/by-nc-nd/4.0/).

Introduction

Total ankle arthroplasty (TAA) is gaining popularity due to the concept that it can provide more functional movements than ankle arthrodesis for reconstruction of degenerative ankles with end-stage arthritis. However, clinical reports have indicated a wide range of iatrogenic complications and a low success rate [1,2] in TAA surgeries. Failure rates were reported to range from 10% to 20% within 10 years after surgery [3—10]. Some failures required conversion to ankle arthrodesis [11], and in extreme cases, led to amputation [4].

Surgical failures may be a result of the fact that prostheses cannot totally resemble natural human ankles, which have complex anatomical structures, sophisticated kinematics and intimate interactions and stabilization mechanisms. Sufficient understanding of the biomechanics of TAA is imperative. Previous biomechanical investigations, including gait analyses [12—19], cadaveric experiments [17,20,21] and radiographic observations, provided useful, but insufficient, exploration of the inner foot. Computational methods are featured to provide insight into human bodies and have been widely used in biomechanical observations.

Finite element (FE) models of TAA have been developed and used to investigate the contact pressure and kinematics of the implants during gait [22]; to evaluate the effects of alignment of prosthesis components [23]; to postulate the bone-remodeling process after TAA [24]; to identify the failure mechanism of the polyethylene component [25] and to further investigate other clinical issues under physiological loading conditions [26]. Precisely, an FE model of TAA with the foot—ankle complex was used to investigate plantar pressure and stress distribution in bones in balanced standing [27]. Models constructed in these studies were based on partial foot segments, which were insufficient for observing the biomechanics of the entire foot and ankle. In this study, FE models of an intact foot and a foot with TAA were developed to (1) evaluate the influence of TAA on the foot biomechanics in terms of plantar pressure, joint contact pressure, bone stress distribution and force transmission and (2) investigate the motion and loading distribution of the ankle prosthesis.

Materials and methods

Ethical approval for this project was granted by The Hong Kong Polytechnic University Human Subject Ethics Subcommittee (reference number HSEARS20070115001). The participant who participated in the gait experiment was informed of the experimental procedures and gave written informed consent for the participation in the magnetic resonance image (MRI) scanning, gait experiment and for publishing the case details without disclosing the participant's identity.

Development of finite element models

An FE model of the intact foot [28,29] involving 28 bones, 103 ligaments, plantar fascia, nine groups of extrinsic muscles and a bulk of encapsulated soft tissue was developed (Fig. 1). A female participant, aged 29 years with a body mass of 54 kg and a height of 165 cm, was recruited to acquire the MRI (2 mm slice interval, 3.0T, Siemens, Erlangen, Germany) of the right foot. She claimed to have no history of lower limb injuries or pathologies. Geometries of 28 bones and foot surface were reconstructed from the MRI using Mimics software (Materialise, Leuven, Belgium) and further edited into an FE model using Abaqus software (Dassault Systèmes Simulia Corp., Providence, RI, USA). The interphalangeal joints of the four lesser toes were simplified as a connection using a 2-mm thick soft layer, while other articulations were defined as frictionless surface-to-surface contact with nonlinear contact properties. Ligaments were constructed using tension-only truss elements,

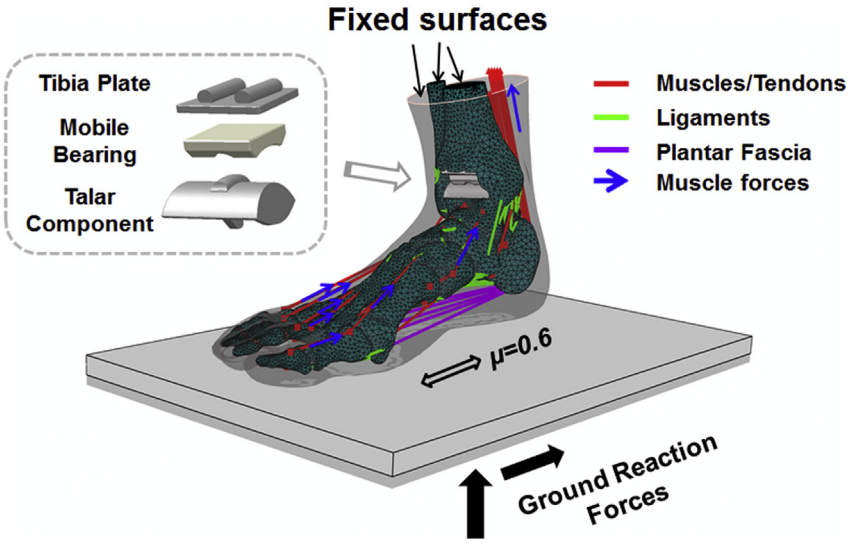

Figure 1 Finite element model of total ankle arthroplasty foot and applications of boundary and loading conditions.

and muscles were represented using axial connector elements that allowed force application.

To obtain the FE model of TAA, the ankle joint in the FE model of the intact foot was resected by the prosthetic ankle, Scandinavian Total Ankle Replacement (STAR, Waldemar Link, Hamburg) prosthesis. Three implant components including a tibia plate, a talar component and a mobile bearing were digitalized and aligned in corresponding positions in the ankle joint based on the guidelines of the surgery, cutting the overlapping ankle bones using Boolean operation, and were fixed to the interface. The bearing component slid between the tibia plate and the talar component with a coefficient of friction of 0.07 [30]. Meshes and material properties of foot segments and implant structures are listed in Table 1.

Boundary and loading conditions

Boundary and loading conditions were obtained from gait analysis of the model subject using Vicon system (Oxford Metrics, Oxford, UK). Reflective markers were attached to the lower limb defining seven body segments to record the motion of the segments and the connecting joints. The participant walked at her natural speed for eight trials, with the feet stepping on individual force platforms (AMTI, Advanced Mechanical Technology, Inc., Watertown, MA, USA) in each trial to record ground reaction forces. Muscle forces were calculated based on electromyography (EMG) signal [39] and muscle cross-section area [40]. Plantar pressure was measured using F-scan (Tekscan Inc., Boston, MA, USA) during the gait analysis for model validation.

Fig. 2 shows ground reaction forces in vertical, mediolateral and anteroposterior directions and the averaged foot-shank angle. Two peaks and a valley occurred in the curve of the vertical ground reaction force, representing the maximum force impacted on the hind and forefoot and full body weight supporting during single-foot support, respectively. These three characteristic instants, namely first-peak (17.5% of the stance phase), mid-stance (48% of the stance phase) and second-peak (76% of the stance phase), were chosen for simulation. To ensure TAA surgery as the exclusive factor in the simulation, the same boundary and loading conditions were applied to the models of both the TAA foot (Fig. 1) and the intact foot.

Table 1 Element type and material properties for segments of the finite element models.

Component	Element type	Young's modulus E (MPa)	Poisson's ratio, v	Cross-section area (mm^2)
Tibia/talar implants [31]	4-node linear tetrahedron	116,000	0.32	—
Mobile bearing implant [32]	4-node linear tetrahedron	8100	0.46	—
Bone [33,34]	4-node linear tetrahedron	7300	0.3	—
Cartilage [35]	4-node linear tetrahedron	1	0.4	—
Ligaments [36]	2-node linear 3-D truss	260	—	18.4
Plantar fascia [37]	2-node linear 3-D truss	350	—	58.6
Ground	8-node linear brick	17,000	0.1	—

Encapsulated soft tissue [38]	4-node linear tetrahedron	C_{10}	C_{01}	C_{20}	C_{11}	C_{02}	D_1	D_2
		0.085	−0.058	0.039	−0.023	0.009	3.652	0.000

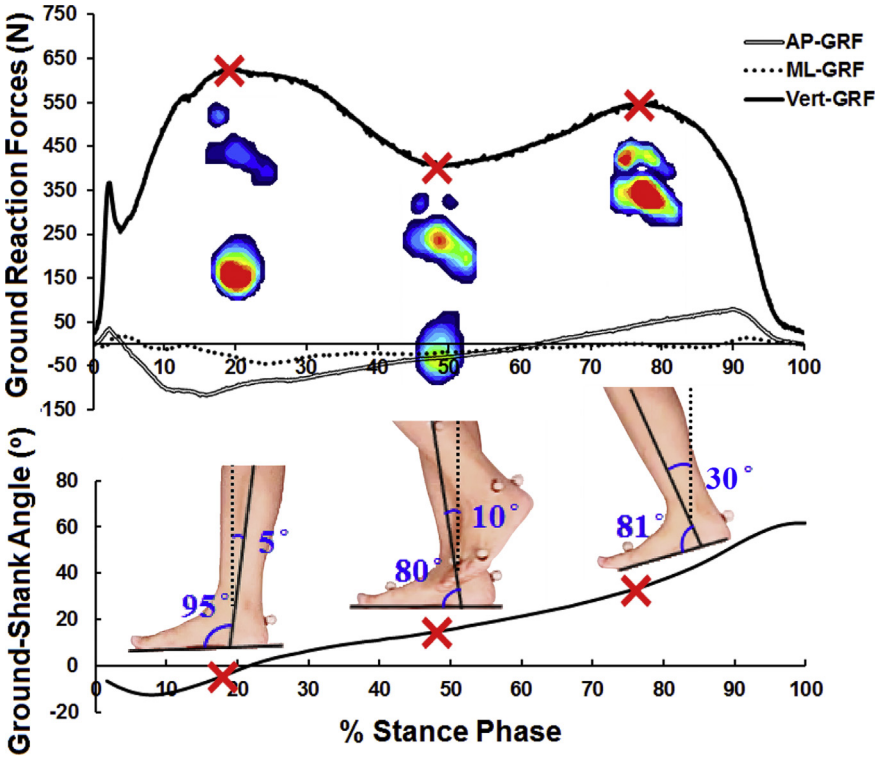

Figure 2 Ground reaction forces (GRF) of the right foot and planar pressure distributions measured during the stance phase of gait. "AP-GRF", "ML-GRF" and "Vert-GRF" mean anteroposterior, mediolateral and vertical ground reaction forces, respectively. Positive for dorsiflexion and negative for plantar flexion in the ground—shank curve.

Model validation

The computational model was validated by plantar pressure measurement and cadaveric experiments. Plantar pressure was measured during the gait trials. A pressure sensor was attached to the plantar foot using double-sided tape. The participant stood upright with the feet apart by a shoulder width for 5 seconds to record the plantar pressure distribution in balanced standing. Plantar pressure distribution during stance phase was recorded during the participant walking. FE-predicted plantar pressure was obtained through the application of boundary and loading conditions to the finite element foot model. Fig. 3 shows the comparison between the two measurements during balanced standing, and at the first-peak and the second-peak instants during gait. There was no observable variation of peak pressure location between the two measurements. In balanced standing, the peak pressure of the forefoot located beneath the heads of the second and third metatarsals and that in the hindfoot located beneath the heel. In the first-peak instant, it located beneath the heel and transferred to the forefoot beneath the first to third metatarsal heads. Deviation of the averaged pressure of the forefoot in balanced standing was less than 15%, and in other cases, it was less than 10%.

A fresh cadaveric right foot and ankle complex was adopted for a mechanical test. The foot and ankle was fixed on a tensile testing machine at the resected end of the distal tibia and fibula bones and was supported by a rotatable plate on the plantar foot. Body weight was applied through compression force from the tension machine. Muscle forces were applied by adding weight to the corresponding tendons. A K-scan (Tekscan Inc) sensor was inserted into the talonavicular joint to measure the joint contact pressure. The cadaver foot was applied with the same loading condition as in FE simulation. The deviation between the experimental measurement and computational prediction was less than 5%.

Results

TAA increased the contact pressure at the medial cuneonavicular joint and bone stress (maximum von Mises stress) in the second and third metatarsals. Forces that transmitted in the medial aspect of the foot were also increased; however, the peak plantar pressure decreased.

The joint motion of the ankle prosthesis in the frontal plane was constrained, which induced a limited range of motion in the sagittal plane. Asymmetric load was predicted such that the lateral aspect of the implants sustained much higher stress than the medial.

Plantar pressure

Fig. 4 shows the plantar pressure distribution in the intact foot model and TAA surgical model. The peak plantar pressure at the first-peak, mid-stance and second-peak instants was 0.260 MPa, 0.553 MPa and 0.605 MPa, respectively, in the TAA foot, which were 21.7%, 19.0% and 11.4%

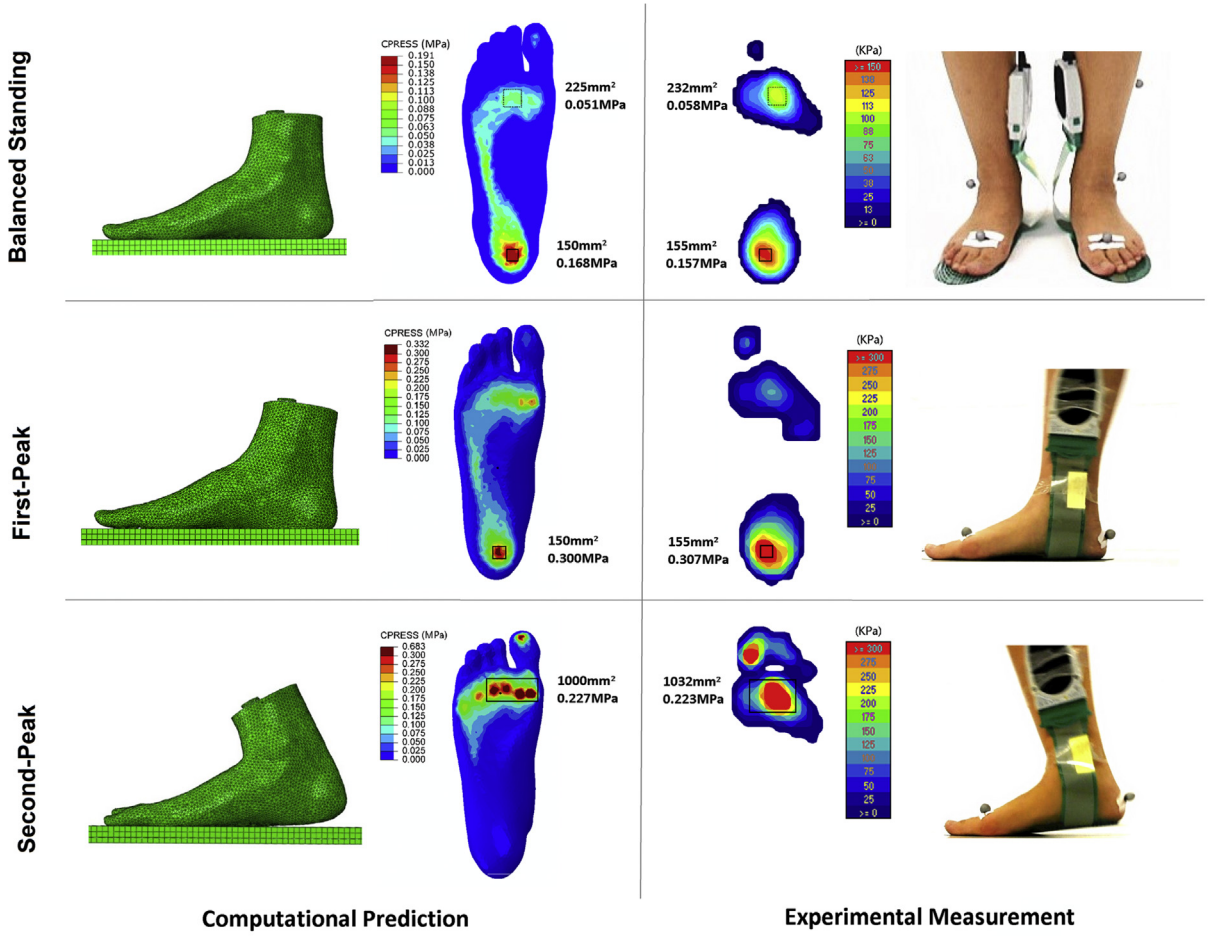

Figure 3 Comparison of plantar pressure between finite element prediction and gait analysis measurement for validation. CPRESS, contact pressure distribution.

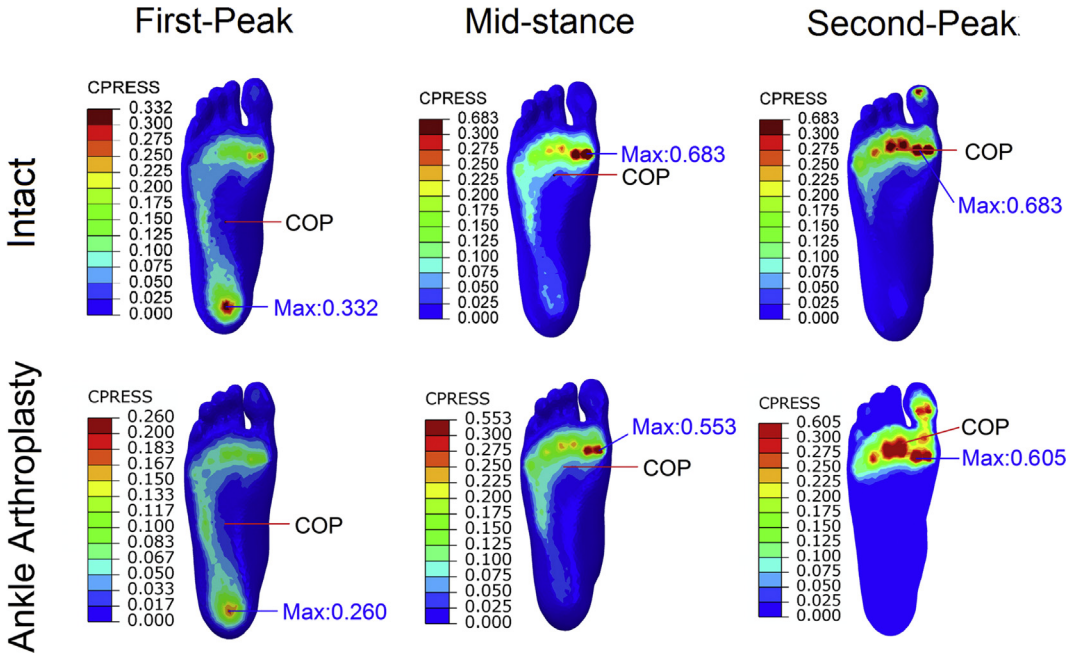

Figure 4 Comparison of the plantar pressure distributions between models of the intact foot and total ankle arthroplasty foot at the first-peak, mid-stance and second-peak instants. COP, center of pressure.

lower than that in the intact foot model. In both anteroposterior and mediolateral directions, the translation of the location of the center of pressure was less than 8 mm at three instants.

Joint contact pressure

Averaged contact pressures in 11 joints in each model were compared, as shown in Fig. 5. The highest pressure occurred in the medial cuneonavicular joint of the TAA foot at the second-peak instant, reaching 3.17 MPa, which was 67.4% higher than that of the intact foot.

The averaged contact pressure at the subtalar joint was 0.35 MPa, 0.52 MPa and 0.72 MPa, respectively, at the three instants in the TAA foot. It decreased by 11%, 3.5% and 7.7% compared with that of the intact foot. In the articulations of the hindfoot and midfoot, consisting of the calcaneocuboid and talonavicular joints, the increase of pressure at the talonavicular joint was less than 1% at the first-peak and mid-stance instants; however, it was 20.5% higher in the TAA foot than that in the intact foot at the second-peak instant (2.00 MPa vs. 2.41 MPa). In the five tarsometatarsal joints, connecting the midfoot and forefoot, the TAA foot sustained 44.0% higher pressure than the intact foot at the second-peak instant except for the fifth tarsometatarsal joint.

Force transmission

In the articulations between the hindfoot and midfoot in the TAA model, the majority of forces transmitted through the talonavicular joint, which were 177 N, 285 N and 618 N, respectively, at the three instants. They were 2.4% lower and 10.1% and 20.3% higher than the corresponding values in the intact foot at the three instants, respectively. The forces transmitted from the midfoot to the forefoot mainly through the first three tarsometatarsal joints, among which the first tarsometatarsal joint sustained larger contact forces in the TAA foot model than in the model of the intact foot. The contact force in this joint was 39 N, 70 N and 236 N, respectively, at the three instants, which was 36.9% and 25.0% lower at the first-peak and mid-stance instants and 18.3% higher at the second-peak instant than that in the intact foot model.

Among the three cuneonavicular joints in the midfoot of the TAA model, the medial one supported the largest contact force throughout the gait. The values of the force were 33 N, 71 N and 249 N, respectively, at the three instants and 45.2% and 25.9% lower and 33.9% higher than those of the intact foot, respectively. In the hindfoot of the TAA model, contact force in the subtalar joint was 134 N, 201 N and 304 N, respectively, at the three instants. It was 18.0%,

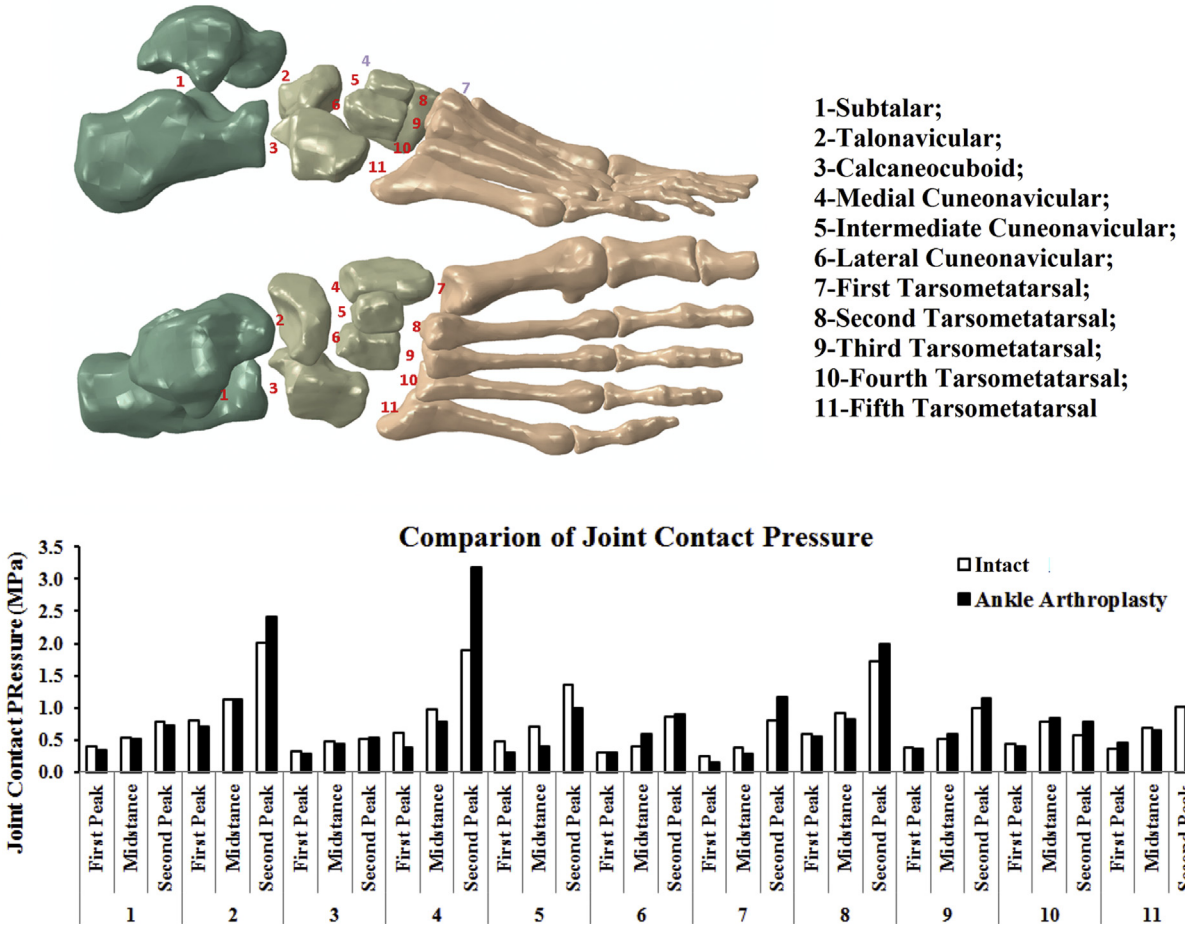

Figure 5 Comparison of joint contact pressure between models of the intact foot and total ankle arthroplasty foot at the first-peak, mid-stance and second-peak instants.

13.3% and 18.5% lower than the corresponding values in the intact foot model, respectively, at the three instants.

Fig. 6 shows the force transmission (in terms of times of body weight) from the hindfoot to the forefoot. Forces transmitted through the lateral path did not vary apparently between the two foot models, whereas more obvious changes occurred in the medial path at the mid-stance and second-peak instants. In total, forces that were 0.48 and 0.95 times the body weight transmitted through the medial way in the intact foot, respectively, at the mid-stance and second-peak instants, and this increased to 0.53 and 1.15 times the body weight in the TAA foot.

Stress in metatarsal bones

The maximum von Mises stress (Fig. 7) was located in the second metatarsal, and was 20.4 MPa, 30.6 MPa and 55.3 MPa, respectively, at three instants in the TAA foot. Compared with the model of the intact foot, the variation was subtle at the first-peak instant but increased by 19.8% and 31.2%, at the mid-stance and second-peak instants, respectively. Another notable deviation between the foot models was that the first metatarsal sustained higher stress in the TAA foot than in the intact foot at the second-peak instant.

Prosthetic joint motion and loading

Motions of the prosthetic ankle were investigated (Fig. 8). In the sagittal plane, it rotated by 2.5°, 4° and 3.5°, respectively, at the first-peak, mid-stance and the second-peak instants. Rotation did occur in the transverse plane but restricted in the frontal plane. Asymmetric loading was exerted in the prosthetic joints, such that the lateral side of the bearing component sustained higher stress than the medial side. The stress at the lateral side of the bearing component was 17.2 MPa, 25.4 MPa and 67.6 MPa at the three instants, respectively.

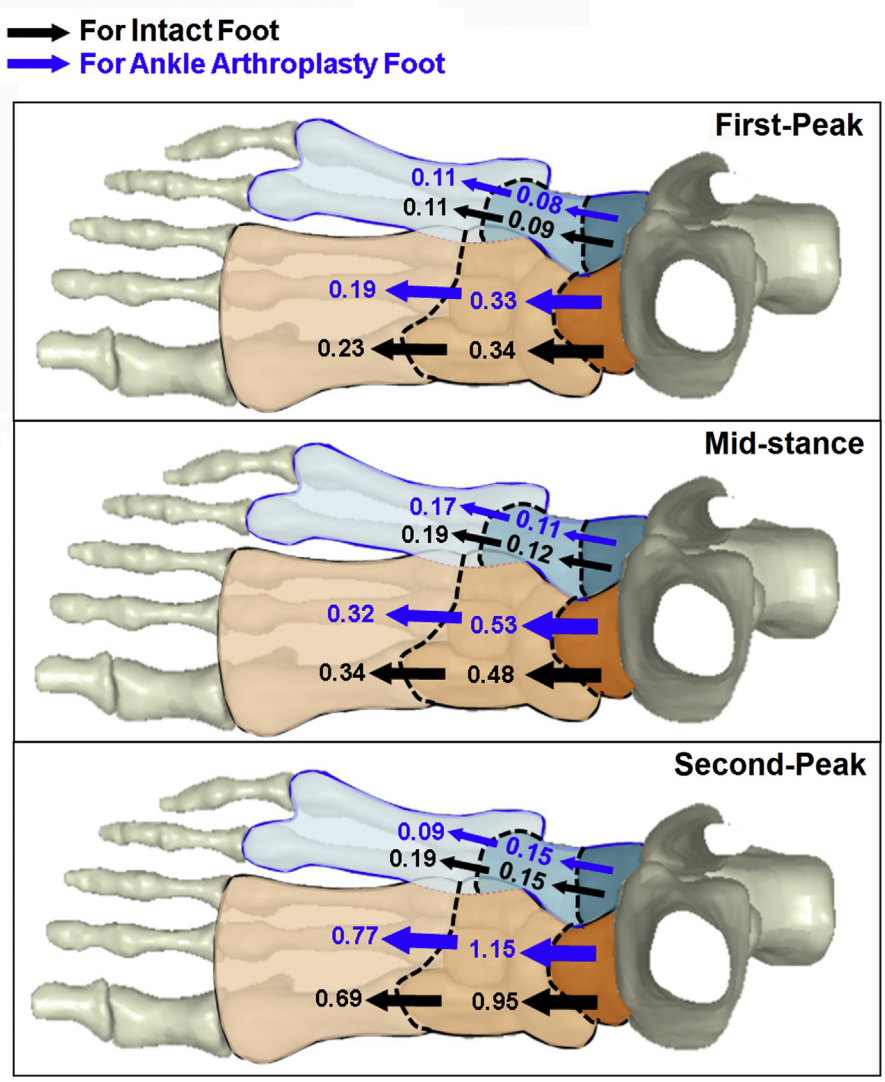

Figure 6 Comparison of force transmission in models of the intact foot and total ankle arthroplasty foot at the first-peak, mid-stance and second-peak instants. Force is depicted in terms of times of body weight. Black arrows are for intact foot, and blue ones are for total ankle arthroplasty foot.

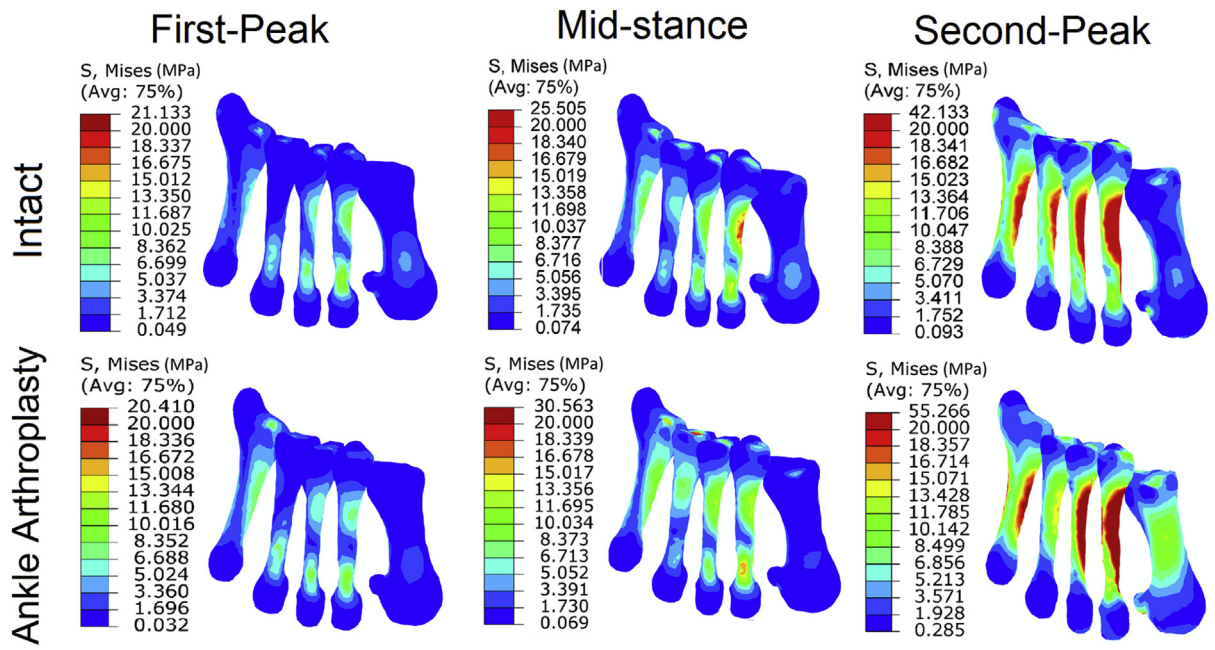

Figure 7 Comparison of von Mises stress distribution in metatarsals between models of the intact foot and total ankle arthroplasty foot at the first-peak, mid-stance and second-peak instants.

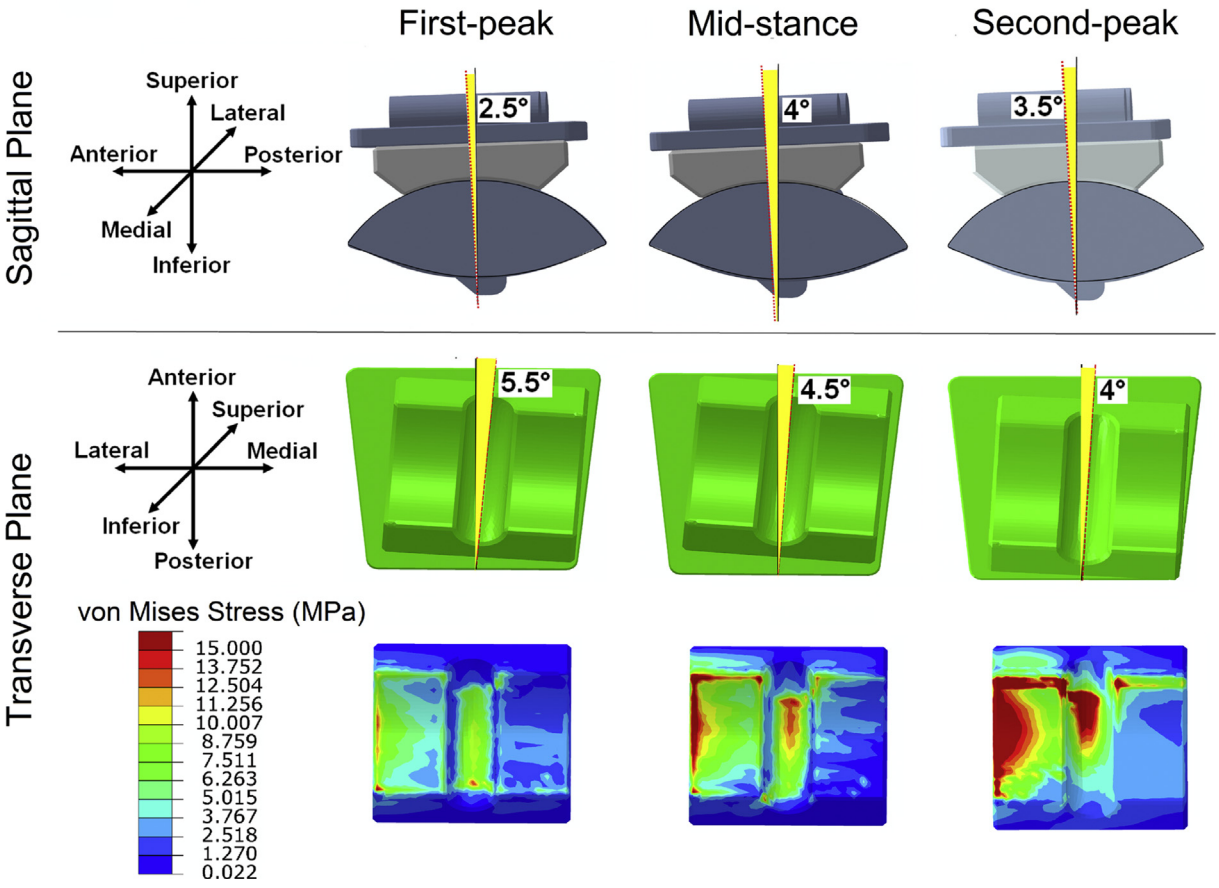

Figure 8 Motion of the prosthetic ankle joint in sagittal planes and the stress distribution in the bearing component.

Discussion

The emergence of TAA allows the retention of the ankle joint for patients with end-stage ankle arthritis, but its complications may hinder the advantages of this intervention. In this study, the biomechanical effects of this surgery on the foot were evaluated based on validated computational models of the foot and ankle, and the joint motion and loading distribution of the ankle prosthesis were also investigated. This surgery technique has predicted and demonstrated alteration of the joint contact pressure, bone stress and force transmission patterns of the foot. Asymmetric loading was induced in the implants.

The three-component design of the ankle prosthesis allows joint motion in the sagittal and transverse planes, while inversion/eversion motion in the frontal plane is structurally constrained. As found in this study, transition and internal/external rotation in the transverse plane occurred, but the range of motion was smaller than that in an intact ankle [41]. The prosthetic ankle is theoretically capable to cover the full range of motion in the sagittal plane as found in an intact foot. However, this rotation in this study was found to be smaller than in the intact foot, which may limit the motion of dorsiflexion due to the coupling effect. This finding verified results in gait analysis studies that dorsiflexion was reduced in TAA patients [11—13,42], which was clinically compensated by Achilles tendon lengthening [11].

Eversion moment at the ankle joint existed during most part of the stance phase [43]; Resistance of this motion resulted in mediolateral asymmetric loading distribution in the bearing component, such that the lateral side sustained much higher loading than the medial side. The asymmetric loading might be a potential indication of fracture of the bearing component [44] and/or talus subsidence or migration [45—47]. Optimization of prosthetic ankle designs to permit rotation in the frontal plane could be a fundamental solution for insufficient dorsiflexion.

Plantar pressure is employed in clinical practice and rehabilitation for the identification of plantar foot disorders. The plantar pressure distribution was found not to be affected by TAA surgery. This was consistent with the results of other biomechanical studies [48]. The anteromedial displacement of the center of pressure (COP) can possibly be interpreted as a consequence of variations in the force transmission pattern.

Contact pressure at the talonavicular and the medial cuneonavicular joints increased in the TAA model at the second-peak instant and were higher than that at other joints. Excessive contact pressure at articular interfaces of joints was believed to be a predominant factor of osteoarthritis [49,50]. These two joints might have a potential risk of degeneration, but until now, no clinical reports have clearly pointed out osteoarthritis at these joints.

More forces transmitted medially in the TAA foot at the mid-stance and second-peak instants, which could explain the phenomenon of increased stress in the medial metatarsals.

The second and third metatarsal bones are most commonly affected by stress fractures, and the fracture of the second metatarsal is one of the most common complaints after foot and ankle surgeries [51]. In this study, the two bones bore much higher von Mises stress than the other metatarsal bones. Although the first metatarsal sustained higher stress in the TAA foot than in the intact foot at the second-peak instant, this stress was much lower than that in the second metatarsal.

This study had several limitations. First, computational models were based on simplifications and assumptions. Bones of the FE model were reconstructed without separation of cortical and trabecular components and were assigned as homogeneous, isotropic and linear elastic material. Second, boundary and loading conditions applied to TAA foot were same as those of the intact foot. Considering these limitations, results from this study were expected to qualitatively analyse the biomechanical effects of TAA from a theoretical perspective, rather than an exact representation of this surgery. Further studies should include motion analysis on TAA patients and application to FE simulations to improve this condition.

Total ankle arthroplasty induced increased loadings in the medial cuneonavicular joint and the second and third metatarsals and forces that transmitted from the first ray. These findings have implications for more extensive attention to patients with foot problems in these regions. The ankle prosthesis bore asymmetric loading, such that the stress on the lateral aspect was much higher than the medial. Prosthesis optimization in terms of joint motion in the frontal plane might be beneficial for a more accurate representation of human ankle joint. All these findings should be further validated by clinical evidence.

Conflicts of interest

All authors declare that they have no conflict of interest.

Funding

This work was supported by the Hong Kong Research Grant Council GRF [PolyU152216/14E, PolyU152002/15E, PolyU152065/17E], National Natural Science Foundation of China NSFC [11732015] and Shenzhen Research Fund [JCYJ-20160531-18462-1718].

References

[1] Spirt AA, Assal M, Hansen ST. Complications and failure after total ankle arthroplasty. J Bone Joint Surg Am 2004;86A(6):1172—8 [English].

[2] Criswell BJ, Douglas K, Naik R, Thomson AB. High revision and reoperation rates using the Agility™ Total Ankle System. Clin Orthop Relat Res 2012;470(7):1980—6 [English].

[3] Knecht SI, Estin M, Callaghan JJ, Zimmerman MB, Alliman KJ, Alvine FG, et al. The agility total ankle arthroplasty - seven to sixteen-year follow-up. J Bone Joint Surg Am 2004;86A(6):1161—71 [English].

[4] Haddad SL, Coetzee JC, Estok R, Fahrbach K, Banel D, Nalysnyk L. Intermediate and long-term outcomes of total ankle arthroplasty and ankle arthrodesis - a systematic review of the literature. J Bone Joint Surg Am 2007;89A(9):1899—905 [English].

[5] Henricson A, Skoog A, Carlsson A. The Swedish ankle arthroplasty register - an analysis of 531 arthroplasties between 1993 and 2005. Acta Orthop 2007;78(5):569—74 [English].
[6] Gougoulias N, Khanna A, McBride DJ, Maffulli N. How successful are current ankle replacements? A systematic review of the literature. Clin Orthop Relat Res 2010;468(1):199—208 [English].
[7] Karantana A, Hobson S, Dhar S. The Scandinavian Total Ankle Replacement survivorship at 5 and 8 years comparable to other series. Clin Orthop Relat Res 2010;468(4):951—7 [English].
[8] Wood PLR, Karski MT, Watmough P. Total ankle replacement: the results of 100 Mobility Total Ankle Replacements. J Bone Joint Surg Br 2010;92B(7):958—62 [English].
[9] Bonnin M, Gaudot F, Laurent JR, Ellis S, Colombier JA, Judet T. The Salto Total Ankle Arthroplasty survivorship and analysis of failures at 7 to 11 years. Clin Orthop Relat Res 2011;469(1):225—36 [English].
[10] Hsu AR, Haddad SL, Myerson MS. Evaluation and management of the painful total ankle arthroplasty. J Am Acad Orthop Sur 2015;23(5):272—82 [English].
[11] Anderson T, Montgomery F, Carlsson A. Uncemented STAR total ankle prostheses. Three to eight-year follow-up of fifty-one consecutive ankles. J Bone Joint Surg Am 2003;85-A(7):1321—9.
[12] Brodsky JW, Polo FE, Coleman SC, Bruck N. Changes in gait following the Scandinavian Total Ankle Replacement. J Bone Joint Surg Am 2011;93A(20):1890—6 [English].
[13] Ingrosso S, Benedetti MG, Leardini A, Casanelli S, Sforza T, Giannini S. GAIT analysis in patients operated with a novel total ankle prosthesis. Gait Posture 2009;30(2):132—7 [English].
[14] Valderrabano V, Nigg BM, von Tschamer V, Stefanyshyn DJ, Goepfert B, Hintermann B. Gait analysis in ankle osteoarthritis and total ankle replacement. Clin Biomech 2007;22(8):894—904 [English].
[15] Jastifer J, Coughlin MJ, Hirose C. Performance of total ankle arthroplasty and ankle arthrodesis on uneven surfaces, stairs, and inclines: a prospective study. Foot Ankle Int 2015;36(1):11—7 [English].
[16] Caravaggi P, Lullini G, Leardini A, Berti L, Vannini F, Giannini S. Functional and clinical evaluation at 5-year follow-up of a three-component prosthesis and osteochondral allograft transplantation for total ankle replacement. Clin Biomech 2015;30(1):59—65 [English].
[17] Flavin R, Coleman SC, Tenenbaum S, Brodsky JW. Comparison of gait after total ankle arthroplasty and ankle arthrodesis. Foot Ankle Int 2013;34(10):1340—8 [English].
[18] Brodsky JW, Coleman SC, Smith S, Polo FE, Tenenbaum S. Hindfoot motion following STAR total ankle arthroplasty: a multisegment foot model gait study. Foot Ankle Int 2013;34(11):1479—85 [English].
[19] Conti S, Lalonde KA, Martin R. Kinematic analysis of the agility total ankle during gait. Foot Ankle Int 2006;27(11):980—4 [English].
[20] Natsakis T, Burg J, Dereymaeker G, Vander Sloten J, Jonkers I. Extrinsic muscle forces affect ankle loading before and after total ankle arthroplasty. Clin Orthop Relat Res 2015;473(9):3028—37 [English].
[21] Fukuda T, Haddad SL, Ren YP, Zhang LQ. Impact of talar component rotation on contact pressure after total ankle arthroplasty: a cadaveric study. Foot Ankle Int 2010;31(5):404—11 [English].
[22] Reggiani B, Leardini A, Corazza F, Taylor M. Finite element analysis of a total ankle replacement during the stance phase of gait. J Biomech 2006;39(8):1435—43 [English].
[23] Espinosa N, Walti M, Favre P, Snedeker JG. Misalignment of total ankle components can induce high joint contact pressures. J Bone Joint Surg Am 2010;92A(5):1179—87 [English].
[24] Bouguecha A, Weigel N, Behrens BA, Stukenborg-Colsman C, Waizy H. Numerical simulation of strain-adaptive bone remodelling in the ankle joint. Biomed Eng Online 2011;10:58 [English].
[25] Elliot BJ, Gundapaneni D, Goswami T. Finite element analysis of stress and wear characterization in total ankle replacements. J Mech Behav Biomed 2014;34:134—45 [English].
[26] Terrier A, Larrea X, Guerdat J, Crevoisier X. Development and experimental validation of a finite element model of total ankle replacement. J Biomech 2014;47(3):742—5 [English].
[27] Ozen M, Sayman O, Havitcioglu H. Modeling and stress analyses of a normal foot-ankle and a prosthetic foot-ankle complex. Acta Bioeng Biomech 2013;15(3):19—27.
[28] Cheung JTM, Zhang M, Leung AKL, Fan YB. Three-dimensional finite element analysis of the foot during standing - a material sensitivity study. J Biomech 2005;38(5):1045—54 [English].
[29] Wang Y, Li ZY, Wong DWC, Zhang M. Effects of ankle arthrodesis on biomechanical performance of the entire foot. PLoS One 2015;10(7), e0134340 [English].
[30] Godest AC, Beaugonin M, Haug E, Taylor M, Gregson PJ. Simulation of a knee joint replacement during a gait cycle using explicit finite element analysis. J Biomech 2002;35(2):267—75 [English].
[31] Chu T. An investigation on contact stresses of New Jersey Low Contact Stress (NJLCS) knee using finite element method. J Syst Integrat 1999;9(2):187—99.
[32] Miyoshi S, Takahashi T, Ohtani M, Yamamoto H, Kameyama K. Analysis of the shape of the tibial tray in total knee arthroplasty using a three dimension finite element model. Clin Biomech 2002;17(7):521—5 [English].
[33] Gefen A, Megido-Ravid M, Itzchak Y, Arcan M. Biomechanical analysis of the three-dimensional foot structure during gait: a basic tool for clinical applications. J Biomech Eng 2000;122(6):630—9.
[34] Nakamura S, Crowninshield RD, Cooper RR. An analysis of soft tissue loading in the foot—a preliminary report. Bull Prosthet Res 1981;10—35:27—34.
[35] Athanasiou KA, Liu GT, Lavery LA, Lanctot DR, Schenck Jr RC. Biomechanical topography of human articular cartilage in the first metatarsophalangeal joint. Clin Orthop Relat Res 1998;348:269—81 [eng].
[36] Siegler S, Block J, Schneck CD. The mechanical characteristics of the collateral ligaments of the human ankle joint. Foot Ankle 1988;8(5):234—42 [eng].
[37] Wright DG, Rennels DC. A study of the elastic properties of plantar fascia. J Bone Joint Surg Am 1964;46:482—92 [eng].
[38] Lemmon D, Shiang TY, Hashmi A, Ulbrecht JS, Cavanagh PR. The effect of insoles in therapeutic footwear—a finite element approach. J Biomech 1997;30(6):615—20.
[39] Perry J. Ankle foot complex. In: Perry J, editor. Gait analysis: normal and pathological function. Thorofare, NJ: SLACK Incorporated; 1992.
[40] Dul J. Development of a minimum-fatigue optimization technique for predicting individual muscle forces during human posture and movement with application to the ankle musculature during standing and walking. Vanderbilt; 1983.
[41] Close R. Some applications of the functional anatomy of the ankle joint. J Bone Joint Surg Am 1956;38(4):761—81 [English].
[42] Doets HC, van Middelkoop M, Houdijk H, Nelissen RG, Veeger HE. Gait analysis after successful mobile bearing total ankle replacement. Foot Ankle Int 2007;28(3):313—22.
[43] Lee SJ, Hidler J. Biomechanics of overground vs. treadmill walking in healthy individuals. J Appl Physiol 2008;104(3):747—55.

[44] Brunner S, Barg A, Knupp M, Zwicky L, Kapron AL, Valderrabano V, et al. The Scandinavian Total Ankle Replacement long-term, eleven to fifteen-year, survivorship analysis of the prosthesis in seventy-two consecutive patients. J Bone Joint Surg Am 2013;95A(8):711—8 [English].
[45] Doets HC, Brand R, Nelissen RGHH. Total ankle arthroplasty in inflammatory joint disease with use of two mobile-bearing designs. J Bone Joint Surg Am 2006;88A(6):1272—84 [English].
[46] van der Heide HJL, Schutte B, Louwerens JWK, van den Hoogen FHJ, Malefijt MCD. Total ankle prostheses in rheumatoid arthropathy Outcome in 52 patients followed for 1-9 years. Acta Orthop 2009;80(4):440—4 [English].
[47] Pellegrini MJ, Schiff AP, Adams SB, Queen RM, DeOrio JK, Nunley JA, et al. Conversion of tibiotalar arthrodesis to total ankle arthroplasty. J Bone Joint Surg Am 2015;97A(24): 2004—13 [English].
[48] Chopra S, Rouhani H, Assal M, Aminian K, Crevoisier X. Outcome of unilateral ankle arthrodesis and total ankle replacement in terms of bilateral gait mechanics. J Orthop Res 2014;32(3):377—84 [English].
[49] Buckwalter JA, Martin JA. Osteoarthritis. Adv Drug Deliv Rev 2006;58(2):150—67.
[50] Martin JA, Buckwalter JA. Post-traumatic osteoarthritis: the role of stress induced chondrocyte damage. Biorheology 2006; 43(3—4):517—21.
[51] Weatherall JM, Chapman CB, Shapiro SL. Postoperative second metatarsal fractures associated with suture-button implant in hallux valgus surgery. Foot Ankle Int 2013;34(1):104—10 [English].